Dynamics of the central-depleted-well regime in the open Bose-Hubbard trimer

Vittorio Penna
Dipartimento di Scienza Applicata e Tecnologia, Politecnico di Torino, Corso Duca degli Abruzzi 24, I-10129 Torino, Italy and CNISM, u.d.r., Politecnico di Torino, Corso Duca degli Abruzzi 24, I-10129 Torino, Italy
(Received 21 February 2013; published 16 May 2013)

We study the quantum dynamics of the central-depleted-well (CDW) regime in a three-mode Bose Hubbard model subject to a confining parabolic potential. By introducing a suitable set of momentum-like modes we identify the microscopic variables involved in the quantization process and the dynamical algebra of the model. We describe the diagonalization procedure showing that the model reduces to a double oscillator. Interestingly, we find that the parameter-space domain where this scheme entails a discrete spectrum well reproduces the two regions where the classical trimer excludes unstable oscillations. Spectral properties are examined in different limiting cases together with various delocalization effects. These are shown to characterize quantum states of the CDW regime in the proximity of the borderline with classically unstable domains.

DOI: 10.1103/PhysRevE.87.052909 PACS number(s): 05.45.Mt, 03.75.Lm, 03.65.Sq

I. INTRODUCTION

Small-size bosonic lattices have attracted considerable attention in the last decade since they allow the exploration of a rich variety of dynamical behaviors in which macroscopic nonlinear effects are triggered through a few controllable parameters [1–10]. Such systems, formed by small arrays of coupled condensates, are governed by the discrete nonlinear Schrödinger equations

$$i\hbar \dot{z}_j = U|z_j|^2 z_j - T(z_{j+1} + z_{j-1}), \tag{1}$$

where U is the boson interaction, T represents the tunneling amplitude, and $|z_j|^2$ is the population of the condensate at well $j \in [1,M]$ in a M-well lattice. Adopted almost 30 years ago to model small molecular systems and study energy-localization effects [11–13], Eqs. (1) still represent the basic theoretic model for studying the dynamics of solitons and of low-energy excitations in lattices [14–17], where bosons can experience both attractive ($U < 0$) and repulsive ($U > 0$) interactions.

The appealing feature of small-size lattices is that equations (1) involve a number of dynamical variables which is small but sufficient to make the system nonintegrable. Thus, while preserving a character simple enough to allow a systematic analytic approach, mesoscopic lattices display strong dynamical instabilities and a variety of behaviors (including chaos) typically occurring in longer chains. This circumstance has stimulated a considerable interest in revisiting nonlinear behaviors [18,19] first studied at the classical level within the fully quantum environment of bosonic lattices [20–25]. Quantum aspects become relevant for lattices involving low numbers of bosons per well. In this case, a realistic description of microscopic processes is provided by the second-quantized Bose-Hubbard (BH) model [26–28],

$$H = \sum_i \left[\frac{U}{2} n_i(n_i - 1) - v_i n_i\right] - T \sum_i (a_i a_{i+1}^+ + \text{H.c.}), \tag{2}$$

where operators a_i, a_i^+ obey commutators $[a_i, a_\ell^+] = \delta_{\ell i}$ and $n_i = a_i^+ a_i$ are number operators. Equations (1), the semiclassical counterpart of model (2), are easily recovered within both the coherent-state [29,30] and the continuous-variable [31] picture showing how operators a_i, a_i^+ are replaced by complex variables z_i, z_i^*.

Theoretical work on mesoscopic lattices has been mainly focused on the three-well array (trimer), this being the simplest nonintegrable model of this class of systems. Many interesting aspects of *semiclassical* trimer have been explored such as its unstable regimes with both repulsive [2] and attractive [4] interaction U, the emergence of chaos in the presence of parabolic confinement [3], external fields [5] or off-site interactions [8], and discrete breather-phonon collisions [10].

Almost in parallel, the impressive development of laser trapping techniques has made concrete the possibility to engineer small-size arrays whose dynamics is accessible to experiments. The most prominent example is the two-well system (dimer) [32,33] obtained by superposing a (sinusoidal) optical potential on the parabolic potential trapping the condensate. The same scheme should enable the realization of linear chains with an arbitrary number of wells by adjusting the laser wavelength (determining the interwell distance) and the parabolic amplitude.

In this scenario, the study of trimer dynamics provides a privileged standpoint to better understand the quantum counterpart of nonlinearity and instabilities. This issue has been discussed in a series of papers examining the spectral properties of *quantum* trimer [20–22], its description within the phase-variable [23] and the Husimi-distribution [24] pictures, and the inclusion of higher-order quantum correlations within the multiconfigurational Hartree method [25]. Quantum trimer has been also used to model coherent transport with weak interaction [34] and thermalization effects within the Fokker-Planck theory [35]. More recently, the single-depleted-well regime of the trimer has been studied in Ref. [36] to evidence the quantum signature of oscillatory instabilities.

In the same spirit, in this paper, we study the quantum aspects of the single-depleted-well regime for an open trimer trapped in a parabolic potential. Based on previous work [3,37], we aim, in particular, to obtain (i) a satisfactory quantum description of stable macroscopic oscillations characterizing this special regime and to detect (ii) significant effects that distinguish the approach to unstable regimes.

The presence of the parabolic trap results in an effective local potential that favors the occupation of the central well.

Due to the absence of a closed geometry, the translation-invariant single-depleted-well solution of ring trimers reduces, in the present contest, to a stationary solution where the central well is depleted and the lateral condensates exhibit twin populations and coherent (opposite) phases. For this reason the relevant regime will be called a central-depleted-well (CDW) regime. Classically, this is represented by trajectories whose initial conditions are close to the CDW fixed point.

The most part of fixed points of the trimer dynamics, which have the form of collective-mode stationary solutions, feature a strong dependence from interaction parameters. The change of the latter provides various mechanisms whereby one can control the coalescence (or the formation) of fixed-point pairs and, thus, the onset of dramatic macroscopic effects [37]. Unlike the other fixed points, the CDW solution has the special feature to be always present, being independent from the model parameters. This property is advantageous at the experimental level in that the conditions for realizing configurations close to the CDW state appear to be weakly conditioned by the tuning of physical parameters. The semiclassical study of the CDW state has shown how its dynamics displays both stable and unstable regimes. In general, trajectories close to the CDW state exhibit oscillations both of the lateral macroscopically occupied condensates and of the central condensate which typically involves small fractions of the whole population.

The interest for the CDW regime is motivated by its complex, manifold character which, in addition to a well-known, rich scenario of stable and unstable behaviors, features dynamical modes whose character is at the border between the classical and the quantum behavior. We will explore this regime showing that an almost exact description can be achieved.

If the small fraction of the central condensate indeed corresponds to a few-boson population, the semiclassical picture must be replaced by a purely quantum-mechanical approach. Apparently, the only variable that must be quantized is the order parameter of the central well while those pertaining to lateral wells (with many bosons) are expected to maintain their classical form. This possibility is only apparent. In this paper we develop a quantum picture based on replacing some of trimer space modes with collective, momentum-like modes. This alternative formulation of trimer dynamics and, in particular, of the CDW regime allows one to identify the dynamical variables that really feature a quantum behavior. The new description is particularly interesting in that the model we obtain can be diagonalized in an exact way by implementing the *dynamical algebra method* [38].

In Sec. II we review the semiclassical trimer model and its quantum counterpart and propose our alternative description in terms of momentum-like modes. Section III is devoted to obtain the energy spectrum and the eigenstates for the two regimes characterizing the CDW dynamics. The diagonalization is made possible by recognizing that algebra sp(4) is the dynamical algebra of this model. In Sec. IV we discuss the energy-spectrum properties for various limiting cases and highlight the link between the parameter-space regions where the spectrum has a discrete character and the regions corresponding to classically stable oscillations. The occurrence of a continuous spectrum is related to classical instability. Section V further illustrates this aspect by showing how various delocalization effects characterize the approach to classically unstable regions. Section VI is devoted to concluding remarks.

II. TRIMER DYNAMICS IN THE CDW REGIME

For a three-well array including parabolic confinement, Eqs. (1) take the form

$$i\dot{z}_j = U|z_j|^2 z_j - v_j z_j - T z_2\,, \quad j = 1,3, \tag{3}$$

$$i\dot{z}_2 = U|z_2|^2 z_2 - v_2 z_2 - T(z_1 + z_3), \tag{4}$$

where on-site potentials v_j are such that $v_2 > v_1 = v_3$ reflecting the form of the external potential. With no loss of generality one can assume $v_2 = V$ and $v_1 = v_3 = 0$. The relevant semiclassical BH Hamiltonian

$$\mathcal{H} = \frac{U}{2}\sum_{j=1}^{3}|z_j|^4 - V|z_2|^2 - T[z_2^*(z_1+z_3) + \text{c.c.}], \tag{5}$$

where canonical variables z_i obey the canonical Poisson brackets $\{z_m^*, z_n\} = i\delta_{mn}/\hbar$, exhibits a single constant of motion $N = \sum_{i=1}^{3}|z_i|^2$ ($\{N,\mathcal{H}\} = 0$) representing the total boson number. Quantities z_i and $|z_i|^2$ are interpreted, in fact, as the condensate order parameter and the boson population at the ith well, respectively, defined by $z_i = \langle a_i\rangle$ and $|z_i|^2 = \langle n_i\rangle$, in the quantum-classical correspondence with the BH model [39].

Among many interesting regimes, the CDW regime, formed by phase-space trajectories whose initial condition are close to the CDW solution,

$$z_2 = 0\,, \quad z_1 = \sqrt{\frac{N}{2}}\,e^{i\varphi - iut/\hbar} = -z_3, \quad u = \frac{UN}{2}, \tag{6}$$

indeed represents a special case due to its evident independence from interaction parameters U, V, and T. The application of linear-stability analysis to the CDW solution [37] shows that the relevant dynamics features both stable and unstable subregimes depending on the value of $\tau = T/(UN)$ and $v = V/(UN)$. In particular, numerical simulations [37] show that the stable regime displays a regular dynamics with periodic oscillations of the three populations possibly involving different time scales. For initial conditions close to the CDW configuration both the lateral and central populations exhibit small deviations from solution (6), thus confirming the fact that lateral condensates oscillate maintaining their macroscopic character, whereas the central well remains almost empty. Similar to Hamiltonian (5), its quantum counterpart,

$$H = \frac{U}{2}\sum_{j=1}^{3} n_j(n_j - 1) - V n_2 - T[a_2^+(a_1 + a_3) + \text{H.c.}], \tag{7}$$

involves three space modes a_j. Only mode a_2, however, features a true quantum character, modes a_1 and a_3 being related to macroscopic boson populations $\langle n_i\rangle = \langle a_i^+ a_i\rangle \simeq N/2$ for $i = 1,3$. This reasoning is only apparently correct. By introducing the new set of dynamical variables

$$A = \frac{z_1 + z_3}{\sqrt{2}}, \quad B = \frac{z_1 - z_3}{\sqrt{2}}, \quad C = z_2, \tag{8}$$

with nonzero canonical Poisson brackets $\{A^*,A\} = i/\hbar$, $\{B^*,B\} = i/\hbar$, we obtain the trimer equations of motion in the alternative form,

$$i\hbar\dot{A} = \frac{U}{2}(|A|^2 + 2|B|^2)A + \frac{U}{2}B^2A^* - \sqrt{2}TC,$$
$$i\hbar\dot{C} = U|C|^2C - VC - T\sqrt{2}A, \qquad (9)$$
$$i\hbar\dot{B} = \frac{U}{2}(|B|^2 + 2|A|^2)B + \frac{U}{2}A^2B^*,$$

equipped with the constant of motion $N = |A|^2 + |B|^2 + |C|^2$. The ensuing version of the CDW solution is

$$A = 0, \quad C = 0, \quad B = \sqrt{N}\, e^{i\varphi - iut/\hbar}, \quad u = UN/2,$$

showing that the entire boson population is attributed to mode B. In this scenario, trajectories representing small deviations from the previous CDW state involve two "microscopic" modes, namely A and C, whose populations are small with respect to the total boson number N. The only macroscopic quantity is thus the population $|B|^2$ of mode B. Equations (9) makes it evident that the rapid phase oscillations of mode B can be easily removed from the trimer dynamics. By setting

$$A = e^{i\varphi(t)}a, \quad C = e^{i\varphi(t)}c, \quad B = e^{i\varphi(t)}b, \qquad (10)$$

with $b = \sqrt{N} + \xi$ and $\varphi(t) = \varphi - ut, \hbar \equiv 1$, where a, ξ, and c describe small deviations from the CDW state, the motion equations reduce to the linear form

$$i\dot{a} \simeq u\,(a + a^*) - T\sqrt{2}\,c$$
$$i\dot{c} \simeq -(u + V)\,c - T\sqrt{2}\,a \qquad (11)$$
$$i\dot{\xi} \simeq u\,(\xi + \xi^*)$$

if quadratic and cubic terms involving microscopic variables a, ξ, and c are neglected. The effective dynamics of the CDW regime is, thus, driven by the first two equations involving modes a and c, since $\xi + \xi^* = 0$ must be imposed to ensure condition $N =$ const in the time evolution of trimer. Simple calculations show that the Hamiltonian corresponding to Eqs. (11) reads

$$\mathcal{H}_f = \mathcal{H} - uN = -\frac{UN^2}{4} + \frac{UN}{4}(\xi + \xi^*)^2 + \frac{UN}{4}(a + a^*)^2$$
$$- (V + u)\,|c|^2 - \sqrt{2}T\,(a^*c + c^*a). \qquad (12)$$

$\mathcal{H}_f$ can be derived as well from Hamiltonian (5) by substituting variables (10). The time-dependent canonical transformations (10) giving A, B, and C in terms of a, ξ, and c, also show that the canonical structure is preserved, namely that $\{X^*,X\} = i/\hbar$ with $X = a,\xi,c$.

A. The quantum model and its dynamical algebra

The discussion of Appendix A shows how, similar to its classical counterpart $\mathcal{H}$, quantum Hamiltonian (7) can be reduced to the quadratic form

$$H_f \simeq -\frac{U}{4}N^2 + \frac{u}{2}(\xi + \xi^+)^2 + un_A + \frac{u}{2}[A^{+2} + A^2]$$
$$- (V + u)n_C - \sqrt{2}T(A^+C + C^+A).$$

This is achieved by introducing quantum collective modes $A = (a_1 + a_3)/\sqrt{2}$, $B = (a_1 - a_3)/\sqrt{2}$, and $C = a_2$ and implementing a suitable time-dependent unitary transformation $\mathcal{U}_t$ able to eliminate the macroscopic dynamics of mode B described, at the classical level, by factor $e^{i\varphi(t)}$ in Eqs. (10). The crucial point is that in the new scenario quantum modes A, $\xi = B - \sqrt{N}$ and C play the same role of classical modes a, ξ, c in Eqs. (11). Operators A, ξ, and C satisfy the standard commutation relation $[A,A^+] = 1$, $[C,C^+] = 1$ and $[\xi,\xi^+] = 1$. The interesting part of H_f is

$$H_0 \simeq \frac{u}{2}[A^{+2} + A^2 + 2n_A] - (V + u)n_C$$
$$- \sqrt{2}T(A^+C + C^+A),$$

which should characterize the quantum dynamical behavior of CDW-like states. H_0 exhibits an unusual, composite form where, in addition to the standard coupling $A^+C + C^+A$ between bosonic modes, mode A involves a pair of two-boson creation/destruction terms, A^{+2} and A^2, typically causing squeezing effects in atom-photon interaction models of quantum optics. These are also responsible for considerably increasing the complexity of the dynamical algebra of H_0.

One should recall that, given a Hamiltonian H_0, its dynamical algebra is the set of operators D_i forming an algebraic structure, with definite commutators $[D_r,D_s] = if_{rsh}D_h$, based on which H_0 can be expressed as a Hermitian linear combination $H_0 = \sum_i \nu_i D_i$. In the absence of A^{+2} and A^2 the dynamical algebra of H_0 is the spin algebra su(2) formed by generators

$$D_+ = A^+C, \quad D_- = C^+A, \quad D_3 = (n_A - n_C)/2$$

with $[D_3,D_\pm] = \pm D_\pm$ and $[D_+,D_-] = 2D_3$, in the well-known two-boson Schwinger realization. In this case, the diagonalization of $H_0 = \nu_3D_3 + \nu D_+ + \nu^*D_-$ with $\nu_3 \in \mathbb{R}$, $\nu \in \mathbb{C}$ would reduce to perform a simple rotation $S \in$ SU(2) such that $SH_0S^+ = \sqrt{\nu_3^2 + |\nu|^2}\,D_3$, where D_3 is, by definition, the diagonal generator of su(2).

Due to A^{+2} and A^2 the dynamical algebra is the more complex symplectic algebra sp(4), reviewed in Appendix B, involving 10 independent generators. To simplify the diagonalization of H_0 it is advantageous to rewrite it in terms of canonical operators x, y, q, and p defined by

$$x = (A + A^+)/\sqrt{2}, \quad y = -i(A - A^+)/\sqrt{2},$$
$$q = (B + B^+)/\sqrt{2}, \quad p = -i(B - B^+)/\sqrt{2}. \qquad (13)$$

The final form of H_0 is

$$H_0 = u\left[x^2 - \frac{1 + 2v}{2}(q^2 + p^2) - 2\sqrt{2}\tau(xq + yp)\right], \qquad (14)$$

where $u = UN/2$, $v = V/(UN)$, and $\tau = T/(UN)$. Even if we have assumed $V > 0$, reflecting the form of the parabolic-potential profile, we shall consider as well the possibility to realize negative V, representing the presence of a repulsive central potential. In the latter case the three local potentials v_j mimic the Mexican hat profile. The critical value where significant changes are expected is $v = -1/2$, below which $-(1 + 2v)/2$ becomes positive.

III. ENERGY SPECTRUM

Hamiltonian H_0 can be diagonalized by a many-step process where one exploits the knowledge of the transformations of group Sp(4) and, in particular, of the effects of their action on momentum and coordinate operators. Diagonalization is achieved by combining in a suitable way squeezing transformations S_α, standard rotations U_θ, and hyperbolic transformation D_ϕ. The latter belong to group Sp(4), being generated, through the usual Lie-group exponential map, by generators Q_1, J_2, and Q_3, respectively, of sp(4) (see Appendix B).

A. Diagonalization of case $v > -1/2$

In this case H_0 can be diagonalized by a three-step process where the diagonal Hamiltonian can be shown to be given by $H_3 = W H_0 W^+$ with $W = D_\phi U_\theta S_\alpha$.

First step. $S_\alpha = e^{-i\alpha Q_1} = e^{i\alpha(xy-qp)/2}$

$$\begin{aligned} S_\alpha x S_\alpha^+ &= x e^{+\alpha}, \quad S_\alpha y S_\alpha^+ = y e^{-\alpha}, \\ S_\alpha q S_\alpha^+ &= x e^{-\alpha}, \quad S_\alpha p S_\alpha^+ = y e^{+\alpha}, \end{aligned} \tag{15}$$

The action of S_α on Hamiltonian H_0 allows one to get the same coefficient (up to a factor -1) for x^2 and q^2

$$H_1 = S_\alpha H_0 S_\alpha^+ = u\sqrt{s}[x^2 - q^2 - sp^2 - \sigma(xq + yp)]$$
$$\sigma \equiv 2\sqrt{2}\,\tau/\sqrt{s}\,, \quad s = v + 1/2\,.$$

provided the condition $e^{2\alpha} = \sqrt{s}$ defining α is imposed.

Second step. $U_\theta = e^{-2i\theta J_2} = e^{-i\theta(xp-qy)}$

$$\begin{aligned} U_\theta x U_\theta^+ &= xC_\theta + qS_\theta, \quad U_\theta y U_\theta^+ = yC_\theta + pS_\theta, \\ U_\theta q U_\theta^+ &= qC_\theta - xS_\theta, \quad U_\theta p U_\theta^+ = pC_\theta - yS_\theta, \end{aligned} \tag{16}$$

where $C_\theta = \cos\theta$ and $S_\theta = \sin\theta$. Transformation U_θ generates the new Hamiltonian $H_2 = U_\theta H_1 U_\theta^+$, introducing an undefined parameter θ whereby terms depending on xq can be suppressed. This condition is achieved by imposing $2\sin(2\theta) - \sigma\cos(2\theta) = 0$, which provides a complete definition of θ through $\mathrm{tg}(2\theta) = \sigma/2$. As a consequence, the new Hamiltonian takes the form

$$\begin{aligned} H_2 = \frac{u\sqrt{s}}{2\sqrt{4+\sigma^2}}&[(4+\sigma^2)(x^2-q^2) - (2s+\sigma^2)(p^2-y^2) \\ &- s\sqrt{4+\sigma^2}\,(p^2+y^2) + 2(v-3/2)\sigma yp]. \end{aligned}$$

Third step. $D_\phi = e^{2i\phi Q_3} = e^{i\phi(xp+qy)}$

$$\begin{aligned} D_\phi x D_\phi^+ &= xc_\phi + qs_\phi, \quad D_\phi y D_\phi^+ = yc_\phi - ps_\phi, \\ D_\phi q D_\phi^+ &= qc_\phi + xs_\phi, \quad D_\phi p D_\phi^+ = pc_\phi - ys_\phi, \end{aligned} \tag{17}$$

with $c_\theta = \mathrm{ch}\phi$ and $s_\theta = \mathrm{sh}\phi$. This hyperbolic transformation has the property to leave $x^2 - q^2$ and $y^2 - p^2$ unchanged. By acting on the last two terms of H_2 one can exploit parameter ϕ to eliminate term yp in the final Hamiltonian. This is given by $H_3 = D_\phi H_2 D_\phi^+$, which reduces to a linear combination of x^2, q^2, y^2, and p^2 if condition

$$2\mathrm{sh}(2\phi)\,(v+1/2)\sqrt{4+\sigma^2} + (2v-3)\sigma\,\mathrm{ch}(2\phi) = 0$$

is satisfied. The latter condition gives the formula

$$\mathrm{th}(2\phi) = -\frac{(2v-3)\,\sigma}{(2v+1)\sqrt{4+\sigma^2}} \tag{18}$$

whereby s_θ and c_θ can be expressed in terms of the interaction parameters. The final Hamiltonian reads

$$\begin{aligned} H_3 = \frac{u\sqrt{s}}{2\sqrt{4+\sigma^2}}\Big[&(4+\sigma^2)\,x^2 - (4+\sigma^2)\,q^2 \\ &- \left(2s+\sigma^2+\frac{\Delta}{2}\right)p^2 + \left(2s+\sigma^2-\frac{\Delta}{2}\right)y^2\Big], \end{aligned}$$

where

$$\Delta = \frac{4}{\sqrt{v+1/2}}\sqrt{(v+1/2)^3 + 8\tau^2(v-1/2)}\,.$$

In order to ensure that Δ assumes real values, the latter formula requires that $(v+1/2)^3 + 8\tau^2(v-1/2) > 0$. This condition, combined with $v > -1/2$, gives

$$\tau < f(v) \equiv \sqrt{\frac{(v+1/2)^3}{8(1/2-v)}} \quad \text{for} \quad -1/2 < v, \tag{19}$$

which identifies a well-defined portion $\mathcal{D}_+$ of the $v\tau$ parameter space. Curve $\tau = f(v)$, denoted by Γ_+, is represented by the red curve of Fig. 1. Hence, among the four domains visible in Fig. 1, $\mathcal{D}_+$ corresponds to the upper region bounded by Γ_+ from below. For $(v,\tau) \in \mathcal{D}_+$ the present diagonalization scheme assigns a well-defined discrete spectrum to Hamiltonian H_0. Note that, for $v \geqslant 1/2$, no upper limit constraints the range of τ. A second domain exhibiting a discrete spectrum can be found for $v \leqslant -1/2$, which will be identified in the sequel.

The energy spectrum is easily worked out by observing that Hamiltonian H_3 can be rewritten in terms of two harmonic-oscillator Hamiltonians:

$$H_3 = \frac{u\sqrt{s}}{2}\left\{R_-\left(\gamma_x^2 x^2 + \frac{y^2}{\gamma_x^2}\right) - R_+\left(\gamma_q^2 q^2 + \frac{p^2}{\gamma_q^2}\right)\right\}$$

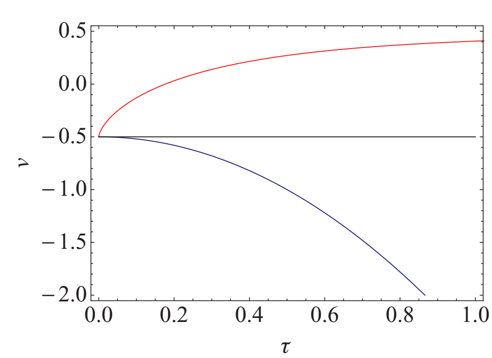

FIG. 1. (Color online) The τv plane features two regions, $\mathcal{D}_+$ and $\mathcal{D}_-$, where the diagonalization process reduces the trimer Hamiltonian to a double-oscillator system with a discrete spectrum. $\mathcal{D}_+$ is the upper domain bounded from below by the red (upper) curve Γ_+ defined by $f(v)$ [see Eq. (19)]. $\mathcal{D}_-$ is delimited by the black straight line Γ_0 ($v = -0.5$) and bounded from below by the blue (lower) curve Γ_- defined by $g(v)$ [see Eq. (27)].

with

$$R_- = \sqrt{2s+\sigma^2-\Delta/2}\,,\quad R_+ = \sqrt{2s+\sigma^2+\Delta/2}$$

(recall that $s = v + 1/2$) and

$$\gamma_x^2 = \sqrt{\frac{4+\sigma^2}{2s+\sigma^2-\Delta/2}}\,,\quad \gamma_q^2 = \sqrt{\frac{4+\sigma^2}{2s+\sigma^2+\Delta/2}}\,. \tag{20}$$

The crucial condition that $2s+\sigma^2-\Delta/2 > 0$ can be easily verified. The eigenstates are defined as product states $|m,n\rangle = \Psi_m(x)\Psi_n(q)$ such that, for each oscillator,

$$\left(\gamma_x^2 x^2 + y^2/\gamma_x^2\right)\Psi_m(x) = (2m+1)\Psi_m(x),$$
$$\left(\gamma_q^2 q^2 + p^2/\gamma_q^2\right)\Psi_n(q) = (2n+1)\Psi_n(q),$$

$\Psi_m(x)$ and $\Psi_n(q)$ being standard harmonic-oscillator eigenfunctions. The resulting spectrum reads

$$E(m,n) = \frac{u\sqrt{s}}{2}\{R_-(2m+1) - R_+(2n+1)\} \tag{21}$$

with $m,n \in \mathbb{N}_0$, and the initial Hamiltonian satisfies the eigenvalue equation $H_0|E(m,n)\rangle = E(m,n)\,|E(m,n)\rangle$ where, in view of the preceding diagonalzation process, one has

$$\begin{aligned} H_0 &= S_\alpha^+ U_\theta^+ D_\phi^+ H_3 D_\phi U_\theta S_\alpha, \\ |E(m,n)\rangle &= S_\alpha^+ U_\theta^+ D_\phi^+ |m,n\rangle. \end{aligned} \tag{22}$$

B. Diagonalization of case $v < -1/2$

In this regime, involving a large central barrier, the diagonalization process can be performed by means of four subsequent steps. These correspond to the four unitary transformations forming $W = D_\phi S_\beta U_2 S_\alpha$ whose action allows one to obtain the new diagonal Hamiltonian $H_4' = W H_0 W^+$. The progressive action of such transformations is discussed in Appendix C. One obtains

$$H_4' = \frac{u\sqrt{w}}{2}\left[\mathcal{R}_+\left(\nu_x^2 x^2 + \frac{y^2}{\nu_x^2}\right) - \mathcal{R}_-\left(\nu_q^2 q^2 + \frac{p^2}{\nu_q^2}\right)\right]$$

with $\mathcal{R}_\pm = \sqrt{\eta^2+2w\pm D}$, $D = 2\sqrt{\eta^2(w+1)+w^2}$,

$$\eta = 2\sqrt{2}\tau/\sqrt{w}\,,\quad w = |v| - 1/2, \tag{23}$$

and

$$\nu_x^2 = \frac{\sqrt{\eta^2-4}}{\sqrt{\eta^2+2w+D}}\,,\quad \nu_q^2 = \frac{\sqrt{\eta^2-4}}{\sqrt{\eta^2+2w-D}}. \tag{24}$$

Similarly to the preceding case where $v > -1/2$, the eigenstates are product states $|k,\ell\rangle = \Phi_k(x)\Phi_\ell(q)$ formed by harmonic-oscillator eigenfunctions such that

$$\left(\nu_x^2 x^2 + y^2/\nu_x^2\right)\Psi_k(x) = (2k+1)\Psi_k(x),$$
$$\left(\nu_q^2 q^2 + p^2/\nu_q^2\right)\Psi_\ell(q) = (2\ell+1)\Psi_\ell(q),$$

The resulting spectrum reads

$$E(k,\ell) = \frac{u\sqrt{w}}{2}\{\mathcal{R}_+(2k+1) - \mathcal{R}_-(2\ell+1)\}. \tag{25}$$

where $k,\ell \in \mathbb{N}_0$. The original Hamiltonian H_0 satisfies the eigenvalue equation $H_0|E(k,\ell)\rangle = E(k,\ell)\,|E(k,\ell)\rangle$, where

$$\begin{aligned} H_0 &= S_\alpha^+ U_2^+ S_\beta^+ D_\phi^+ H_4' D_\phi S_\beta U_2 S_\alpha, \\ |E(k,\ell)\rangle &= S_\alpha^+ U_2^+ S_\beta^+ D_\phi^+ |k,\ell\rangle. \end{aligned} \tag{26}$$

The range of validity of transformations S_α and S_β in terms of parameter v defines the region $\mathcal{D}_-$ of parameter space $v\tau$ in which, for $v < -1/2$, the diagonalization process succeeds. The actions of S_α is well defined if $v < -1/2$ (this ensures that $e^\alpha \in \mathbb{R}$), while S_β, for a given v, requires that $\eta > 2$, namely

$$\tau > g(v), \quad g(v) \equiv \sqrt{|v| - 1/2}/\sqrt{2} \tag{27}$$

(see Appendix C). We will denote curve $\tau = g(v)$ and the straight line $v = -1/2$ with Γ_- and Γ_0, respectively. Thus, domain $\mathcal{D}_-$ corresponds to the region bounded by Γ_- from below and by Γ_0 from above (see the caption of Fig. 1). This result confirms that the regions of plane τv where the current diagonalization scheme is effective correspond to the regions where classical oscillations are stable.

IV. STRUCTURE OF THE ENERGY SPECTRUM AND CLASSICAL INSTABILITY

A. Spectrum of case $v > -1/2$

Domain $\mathcal{D}_+$ described by inequalities (19) reproduces in Fig. 1 the first of the two regions of the stability diagram relevant to the CDW regime [37], in which classical trajectories with initial condition close to the CDW solution are dynamically stable. The property that CDW classical states are stable thus corresponds, quantum mechanically, to the fact that the diagonalization process reduces the system to a simple double oscillator.

The dependence of energy spectrum (21) on parameters τ and v allows one to identify two regimes characterized by the inequalities

$$\tau \ll 1, \quad \Delta \ll 1,$$

respectively, in which the spectrum manifests significant changes. Region $\mathcal{D}_+$ of Fig. 1 shows that, for a given value of v in the interval $[-1/2, 1/2]$, parameter τ ranges in $[0, f(v)]$, where $\tau = f(v)$ defines boundary Γ_+ of $\mathcal{D}_+$. While the first regime corresponds to values of τ close to the vertical axis v (interwell tunneling inhibited), the second regime, where $\Delta \to 0$, corresponds to approaching boundary Γ_+ from the left, namely $\tau \to (f(v))^-$. Thus, $\Delta \to 0$ drives the approach to the region where the classical instability occurs.

1. Regime $\tau \ll 1$

In the weak-tunneling case, by exploiting the Taylor expansion of $R_\pm$ to the second order in τ, one obtains the expression

$$E(m,n) = \frac{u\sqrt{s}}{2}\left[\frac{2\sqrt{2}\,\tau}{s}(2m+1) - R_+(2n+1)\right],$$

with

$$s = \sqrt{v+1/2}\,,\quad R_+ \simeq \sqrt{4s + \frac{16v\,\tau^2}{s^2}},$$

showing that quantum number n describes the large-scale energy changes while quantum number m describes the *fine* *structure* of the spectrum. The reference case, of course, is represented by $E(0,0)$, the energy of the quantum states $|0,0\rangle$ corresponding to the minimum deviation from the pure CDW configuration.

The presence of the parabola, represented by $v > 0$, diminishes the fine-structure level separation with respect to the case $v = 0$ involving no confinement. A more apparent effect occurs for $v < 0$ where the attractive potential of the central well becomes a potential barrier. In this case the fine-structure level separation obtained with small τ is contrasted by factor $1/\sqrt{s}$. Decreasing v by maintaining τ constant shows that such an effect is maximum when one approaches boundary Γ_+ from above.

2. *Regime* $\Delta \ll 1$

The two oscillators tend to become identical ($\gamma_x - \gamma_q \to 0$) and the relevant energy levels are almost indistinguishable. This determines a *macroscopic change* of the energy spectrum of H_0 which becomes visible by effecting, with $|v| < 1/2$, the Taylor expansion of $R_\pm$ in terms of variable Δ. The resulting spectrum has the form

$$E(m,n) = \frac{u\sqrt{s}}{2}\left[2R\,(m-n) - \frac{\Delta\,(m+n+1)}{2R}\right]$$

with $R := \sqrt{2v + 1 + \sigma^2} = R_\pm$ for $\Delta = 0$. Eigenvalues $E(m,n)$ feature a band structure described by $h = m - n$ and a *fine structure* controlled by parameter Δ and the composite quantum number $m + n + 1$. The choice $m = n$ describes the band exhibiting the minimal deviation from the pure CDW configuration.

For $\Delta \to 0$ the fine structure of each band becomes infinitely dense since the interlevel distance tends to zero. In this regime the behaviors of the two oscillators are *strongly correlated* in that small energy changes requires the simultaneous change of m and n in order to preserve h. All the effects described so far disappear at $v = 1/2$ (and, more in general, for $v > 1/2$) since parameter Δ no longer vanishes. Also, the range of τ becomes unlimited consistent with the fact that τ does not cross the unstable-regime boundary Γ_+.

B. Spectrum of case $v < -1/2$

The present regime $v < -1/2$ features as well two significant limiting cases occurring in the proximity of boundaries Γ_- and Γ_0. These are

$$\eta - 2 \ll 1, \quad |v| - 1/2 \ll 1$$

[see definition (23)], which correspond to approaching (i) the curve $g(v)$ from the right, at a given v and (ii) the straight line $v = -1/2$ from below, at a given τ, respectively. Hence, the approach to the regions where the classical instability crops up is driven by either $\eta - 2 \to 0$ or $|v| \to 1/2$.

1. *Regime* $\eta - 2 \ll 1$

One easily checks that $\eta \to 2^+$ amounts to effecting the limit $\tau \to g(v) \equiv \sqrt{w/2}$. By substituting $\tau = \eta\sqrt{w}/(2\sqrt{2})$ in $\mathcal{R}_\pm$, and considering the Taylor expansion in $\eta - 2$, one obtains

$$\mathcal{R}_+ \simeq 2\sqrt{2 + w}\,, \quad \mathcal{R}_- \simeq 2\sqrt{\eta - 2}\,\rho$$

with $\rho = \sqrt{(2w+3)/(w+2)}$ entailing that

$$E(k,\ell) = u\sqrt{w}\,[\sqrt{2+w}\,(2k+1) - \sqrt{\eta-2}\,\rho(2\ell+1)].$$

Quantum number k represents the band index, while the fine structure of the spectrum is controlled by number ℓ. For $\eta \to 2^+$, similar to the case $\tau \to 0$ of Sec. IV A, the spectrum acquires an almost continuous character.

2. *Regime* $|v| - 1/2 \ll 1$

In this case, effecting the limit $v \to (-1/2)^-$ in Eq. (25) implies that

$$E(k,\ell) = u\,[2\sqrt{2}\tau(k-\ell) + \sqrt{w}(k+\ell+1)],$$

where the approximation to the first order in w

$$\sqrt{w}\mathcal{R}_\pm \simeq 2\sqrt{2}\tau\left(1 \pm \frac{\sqrt{w}}{2\sqrt{2}\tau}\right) = 2\sqrt{2}\tau \pm \sqrt{w}$$

has been used. Spectrum (25) thus undergoes a *macroscopic change* with energy levels forming a band structure described by index $h = k - \ell$ and a w-dependent fine structure described by index $k + \ell$. The separation between two subsequent levels tends to zero for $w \to 0$. Transitions in which $k \to k + r$, $\ell \to \ell + r$ are thus favored in that small energy changes are involved. Similarly to the case $\Delta \ll 1$ of Sec. IV A, the two oscillators appear to be *strongly correlated* in that $\Delta k \equiv \Delta\ell$.

C. Transition to a continuous spectrum

Transformations $W = D_\phi U_\theta S_\alpha$ and $W = D_\phi S_\beta U_2 S_\alpha$ [see formulas (22) and (26), respectively] no longer work at the boundaries Γ_+, Γ_0, and Γ_- of the relevant stability domains. In particular, in the case $v > -1/2$, the action of D_ϕ in W is defined for arbitrarily large values of ϕ as shown by Eq. (18). The latter shows that $\mathrm{th}(\phi) \to 1$ for $\tau \to f(v)$ meaning that Γ_+ is approached (but not reached) from below. Likewise, for $v < -1/2$, the range of parameters α and β (see Appendix C) relevant to S_α and S_β, respectively, allows one to get closer and closer to boundaries Γ_0 and Γ_- without reaching them.

At such boundaries the spectrum displays a structural change corresponding to the fact that the diagonalization of H_0 yields an operator pertaining to a sector of the dynamical algebra disjoint from the one where H_0 reduces to a simple two-oscillator model. In the new sector the discrete character of the spectrum is lost. A paradigmatic example of such an effect is supplied by the harmonic oscillator with time-dependent parameters [40].

Hamiltonian H_0 at the boundary Γ_0 where $v \equiv -1/2$ well exemplifies this situation. In this case, H_0 reduces to $H_0 = u[x^2 - 2\sqrt{2}\tau(xq + yp)]$. The action of transformation $M = e^{-i\varphi xp}$ on H_0 giving $H_0' = MH_0M^+$ followed by the unitary transformation $x \to y$, $y \to -x$ takes H_0 into the form

$$H_0'' = u\left[\tfrac{1}{2}(y^2 + p^2) - g(xp - yq)\right],$$

which exhibits the two-dimensional Laplacian $y^2 + p^2$ together with the generator $L_3 = xp - yq$ of planar rotations. After noting that such operators commute with each other, one easily observes that, despite that L_3 has a discrete spectrum, the energy spectrum features a continuous character due to the presence of Laplacian. Since the same result can be shown to occur at boundaries Γ_- and Γ_0, then we conclude that at the border separating (classically) stable from unstable regimes the energy spectrum acquires a continuous character.

The correct interpretation of such an effect is twice. At the boundaries Γ_+, Γ_-, and Γ_0 of $\mathcal{D}_\pm$ the approximation inherent in model (14), involving microscopic modes A and C, is no longer valid. This is obvious, noting that the spectrum of quantum trimer is discrete by definition. The onset of a continuous spectrum is, thus, an artifact of the momentum-mode picture when this is used outside its domains of validity $\mathcal{D}_\pm$. On the other hand, the emergence of a continuous spectrum just amplifies the effect observed in the proximity of Γ_+, Γ_-, and Γ_0, which consists in the vanishing of energy-level separation (see Secs. IV A and IV B). In this sense, the continuous spectrum is a dramatic manifestation of the transition to the classically unstable regions.

V. DELOCALIZATION EFFECTS

The discussion of Secs. IV A and IV B shows that both regimes $v > -1/2$ and $v < -1/2$ feature limiting cases where a suitable choice of parameters v and τ allows one to approach the boundaries of the domains classically involving stable oscillations. The significant change of the spectrum structure observed in such cases is accompanied by a dramatic change of the localization properties of the system. To see this one must consider deviations $\Delta_f^2 = \langle f^2(t)\rangle - \langle f(t)\rangle^2$, where f represents one of canonical operators x, y, q, and p, and

$$\langle f^r(t)\rangle = \langle E|f^r(t)|E\rangle = \langle E|R^+ f^r R|E\rangle,$$

with $r = 1,2$. The action of propagator $R = e^{-itH_0/\hbar}$ on energy eigenstates $|E\rangle$ allows one to considerably simplify this calculation. Formulas (22) and (26) show that $H_0 = W^+ H_d W$ and $|E(\Omega)\rangle = W^+|\Omega\rangle$ in which

$$W = D_\phi U_\theta S_\alpha, \quad W = D_\phi S_\beta U_2 S_\alpha.$$

In the two cases $v > -1/2$ and $v < -1/2$, one has $H_d = H_3$, $H_d = H_4'$, and $|\Omega\rangle = |m,n\rangle$, $|\Omega\rangle = |k,\ell\rangle$, respectively. As a consequence, the calculation of expectation values $\langle f^r(t)\rangle$ reduces to

$$\langle\Omega|W\,R^+ f^r R\,W^+|\Omega\rangle = \langle\Omega|W\,f^r\,W^+|\Omega\rangle,$$

with $H_0 = W^+ H_d W$ in propagator $R(t)$. One easily shows that $\langle\Omega|\,W f W^+|\Omega\rangle = 0$ so the determination of Δ_f^2 amounts to calculating

$$\Delta_f^2 = \langle n,m|D_\phi U_\theta S_\alpha\, f^2 S_\alpha^+ U_\theta^+ D_\phi^+|m,n\rangle,$$

$$\Delta_f^2 = \langle \ell,k|D_\phi S_\beta U_2 S_\alpha\, f^2 S_\alpha^+ U_2^+ S_\beta^+ D_\phi^+|k,\ell\rangle,$$

with $f = x,y,q,p$. The derivation of such formulas is discussed in Appendix D.

Let us consider, first, the approach to boundary Γ_+ characterized by $\Delta \simeq 0$. In the proximity of Γ_+ one finds that $\tau^2 \simeq f^2(v) = s^3/[8(1-s)]$ and $\sigma^2 \simeq s^2/(1-s)$ while $R_\pm \simeq R = (2s+\sigma^2)^{1/2}$ and $F_\pm \simeq F = s(2-s)$. Hence, equations (D1) and (D2) reduce to

$$\Delta_x^2 \simeq \frac{2R^3\sqrt{s}}{(4+\sigma^2)\Delta}(m+n+1), \quad \Delta_y^2 \simeq \frac{2F}{R\sqrt{s}\Delta}(m+n+1),$$
$$\Delta_q^2 \simeq \frac{2RF\,(m+n+1)}{(4+\sigma^2)\sqrt{s}\Delta}, \quad \Delta_p^2 \simeq \frac{2R\sqrt{s}}{\Delta}(m+n+1),$$

clearly showing how such squared deviations diverge due to the factor $1/\Delta$. For $s \geqslant 1$ ($\leftrightarrow v \geqslant 1/2$) parameter Δ no longer vanishes whatever value is assumed by τ. The delocalization effect is, thus, restricted to neighborhood of Γ_+.

Concerning the boundaries of $\mathcal{D}_-$, the approach to Γ_- (blue curve in Fig. 1) discloses a somewhat different diverging behavior of squared deviations Δ_f^2. In particular, based on formulas (D3), (D4), and (D5), one gets

$$\Delta_x^2 \simeq \frac{(2\ell+1)\sqrt{w}}{2\sqrt{\epsilon}\sqrt{w+2}}, \quad \Delta_y^2 \simeq \frac{(2k+1)}{4\sqrt{w(w+2)}},$$
$$\Delta_q^2 \simeq \frac{(2\ell+1)}{2\sqrt{\epsilon}\sqrt{w(w+2)}}, \quad \Delta_p^2 \simeq \frac{(2k+1)\sqrt{w}}{4\sqrt{w+2}},$$

in the limit $\epsilon = \eta^2 - 4 \to 0$, where factor $1/\sqrt{\epsilon}$ is responsible for the delocalization effect. The latter affects only position operators x and q without involving y and p.

Finally, the limit $w \to 0$, describing the approach to the straight line Γ_0 defined by $v = -1/2$, supplies a third interesting situation. In this case,

$$\Delta_x^2 = \Delta_p^2 \simeq \frac{\sqrt{w}}{2}(k+\ell+1), \quad \Delta_y^2 = \Delta_q^2 \simeq \frac{k+\ell+1}{2\sqrt{w}},$$

involve an evident squeezing effect where the delocalization issuing from Δ_y^2 and Δ_q^2 is compensated by the localization effect concerning Δ_x^2 and Δ_p^2, respectively.

VI. CONCLUSIONS

We have studied the quantum-mechanical properties of the Bose-Hubbard trimer in the CDW regime. The interesting feature of this regime is that it exhibits both stable and unstable (classical) regimes whose dependence on interaction parameters is completely known. This has given us the possibility to study the relation between the stability character of trimer and its quantum properties.

In Sec. II, we have introduced an alternative description in terms of momentum-like modes which allows one to identify the classical (microscopic) variables involved by the quantization process. In Sec. III we have enacted the procedure for diagonalizing the trimer Hamiltonian based on the knowledge of the model dynamical algebra. Within the momentum-mode picture, this is found be the algebra sp(4).

The implementation of this procedure reduces the model to a double-oscillator system and allows us to identify the regions $\mathcal{D}_+$ and $\mathcal{D}_-$ where the spectrum is discrete. The nice analytic result emerging from this part is that the derivation of (the boundaries of) $\mathcal{D}_+$ and $\mathcal{D}_-$ exactly reproduces the regions where the trimer is classically stable in the CDW regime.

The discussion of Sec. IV makes evident the significant changes of spectrum structure when approaching the boundary of stability domains $\mathcal{D}_+$ and $\mathcal{D}_-$. Various delocalization effects, discussed in Sec. V, confirm the considerable sensitivity of the quantum properties of the system from the proximity to the boundaries of $\mathcal{D}_+$ and $\mathcal{D}_-$. All such effects can be interpreted as the hallmark of the transition to the unstable regions of classical CDW dynamics whose most dramatic manifestation is the onset of a continuous spectrum when the domain of validity of the momentum-mode picture is left.

Future work will be focused on extending the investigation of the quantum properties of trimer in more complex regimes (such as the dimeric and nondimeric regimes studied in Refs. [3,37]) where the transition to unstable oscillations can be controlled through the model parameters. We hope to include various macroscopic dynamical effects reflecting parameter-dependent structural changes of the phase space so far examined only for the classical trimer [37].

ACKNOWLEDGMENTS

The author thanks P. Buonsante and R. Franzosi for stimulating discussions. This work has been partially supported by the M.I.U.R. project "Collective Quantum Phenomena: From Strongly Correlated Systems to Quantum Simulators" (PRIN 2010LLKJBX).

APPENDIX A: COLLECTIVE-MODE QUANTUM PICTURE

Similar to classical modes (8) the new quantume modes are defined by $A=(a_1+a_3)/\sqrt{2}$, $B=(a_1-a_3)/\sqrt{2}$, and $C=a_2$. By substituting the latter in Hamiltonian (7) and observing that

$$(a_1^+a_1)^2+(a_3^+a_3)^2=\tfrac{1}{2}(n_A+n_B)^2+\tfrac{1}{2}(A^+B+B^+A)^2$$

with $n_A=A^+A$ and $n_B=B^+B$, one finds

$$H=\frac{U}{4}\big[n_A^2+n_B^2+4n_An_B+(A^+)^2B^2+(B^+)^2A^2+2n_C^2+n_A+n_B\big]-\frac{U}{2}N-Vn_C-\sqrt{2}T(A^+C+C^+A).$$

This Hamiltonian must be transformed in order to get the quantum version of $\mathcal{H}_f$. Quantum mechanically, the time-dependent canonical transformation (10) corresponds to unitary transformation $\mathcal{U}_t=\exp[i\varphi(t)N]$ with $\varphi(t)=\varphi-ut/\hbar$ and $N=n_A+n_B+n_C$, whose action takes Hamiltonian $H=H(A,B,C)$ into Hamiltonian $H_f=H-uN$. This result is achieved by changing the Hilbert-space basis through the action of $\mathcal{U}_t$, namely by setting $|\Psi\rangle=\mathcal{U}_t|\Phi\rangle$ in the Schröndinger problem $i\hbar\partial_t|\Psi\rangle=H|\Psi\rangle$ based on the ABC picture. The latter becomes $i\hbar(\partial_t\mathcal{U}_t)|\Phi\rangle+i\hbar\mathcal{U}_t\partial_t|\Phi\rangle=H\mathcal{U}_t|\Phi\rangle$ giving

$$i\hbar\partial_t|\Phi\rangle=[-i\hbar\mathcal{U}_t^+(\partial_t\mathcal{U}_t)+\mathcal{U}_t^+H\mathcal{U}_t]|\Phi\rangle.$$

Then

$$H_f=-i\hbar\mathcal{U}_t^+(\partial_t\mathcal{U}_t)+\mathcal{U}_t^+H\mathcal{U}_t=H+\hbar N\dot{\phi}=H-u\,N,$$

being $[N,H]=0$. The invariance of Hamiltonian H, entailing that $\mathcal{U}_t^+H(A,B,C)\mathcal{U}_t=H(A,B,C)$, directly follows from the transformation formulas

$$\mathcal{U}_tX\mathcal{U}_t^+=Xe^{-i\varphi(t)},\quad X=A,B,C. \tag{A1}$$

The action described by (A1) is equivalent to introducing a, b, and c within the classical description. Conversely, the latter are not required in the quantum picture since transformations (A1) introduce in a direct way the time-dependent exponential factor $e^{-i\varphi(t)}$. In the present scheme, for example, the expectation values $\langle\Psi|A|\Psi\rangle$ (relevant to the dynamics governed by H) and $\langle\Phi|A|\Phi\rangle$ (relevant to the dynamics governed by H_f) correspond to the classical variables A and a, respectively, since

$$\langle\Psi|A|\Psi\rangle=\langle\Phi|\mathcal{U}_t^+A\,\mathcal{U}_t|\Phi\rangle=e^{i\varphi}\langle\Phi|A|\Phi\rangle.$$

The last step consists in replacing B with $\sqrt{N}+\xi$. The substitution of the latter in n_B and n_B^2 gives $n_B=N+\sqrt{N}(\xi+\xi^+)+\xi^+\xi$ and

$$\begin{aligned}n_B^2&=(N+\sqrt{N}(\xi+\xi^+)+\xi^+\xi)^2\\&\simeq N^2+N(\xi+\xi^+)^2+2N\sqrt{N}(\xi+\xi^+)+2N\xi^+\xi,\end{aligned} \tag{A2}$$

where terms such as $(\xi^+\xi)^2$, $\xi^2\xi^+$, and $(\xi^+)^2\xi$ have been neglected. This omission is justified by the fact that mode ξ, as well as A and C, represent weakly populated modes. Hence, the expectation values of $(\xi^+\xi)^2$ and $\xi^2\xi^+$ represent pertubative terms that can be neglected. For the same reason terms $(A^+)^2B$ and A^2B^+ can be eliminated as well as terms n_A^2 and n_C^2. Then H_f reduces to

$$H_f\simeq\frac{U}{4}\big[n_B^2+4n_An_B+B^2(A^+)^2+A^2(B^+)^2\big]-u(n_A+n_B+n_C)-Vn_C-\sqrt{2}T(A^+C+C^+A),$$

since $U(n_A+n_B+n_C)/2$ and $U(n_A+n_B)/4$ are negligible with respect to $u(n_A+n_B+n_C)$, being $u=UN/2\gg U$. Implementing the substitution $B=\sqrt{N}+\xi$ gives

$$H_f\simeq-\frac{u}{2}N+u(\xi+\xi^+)^2+un_A+\frac{u}{2}[(A^+)^2+A^2]-(V+u)n_C-\sqrt{2}T(A^+C+C^+A).$$

APPENDIX B: CANONICAL FORM OF ALGEBRA sp(4)

By expressing bosonic operators in terms of canonical variables $A=(x+iy)/\sqrt{2}$ and $C=(q+ip)/\sqrt{2}$ the canonical version of algebra sp(4) is given by

$$\begin{aligned}J_1&=\frac{A^+C+C^+A}{2}=\frac{xq+yp}{2}\\J_2&=\frac{A^+C-C^+A}{2i}=\frac{xp-qy}{2}\\J_3&=\frac{A^+A-C^+C}{2}=\frac{x^2+y^2-q^2-p^2}{4}\\J_0&=\frac{A^+A+C^+C+1}{2}=\frac{x^2+y^2+q^2+p^2}{4}\end{aligned} \tag{B1}$$

$$\begin{aligned}K_3&=\frac{CA+A^+C^+}{2}=\frac{xq-yp}{2}\\K_2&=\frac{A^2-A^{+2}+C^2-C^{+2}}{2i}=\frac{xy+yx+qp+pq}{4}\\K_1&=\frac{C^2+C^{+2}-A^2-A^{+2}}{2}=-\frac{x^2-y^2-(q^2-p^2)}{4}\end{aligned} \tag{B2}$$

$$Q_1 = \frac{A^{+2} - A^2 + C^2 - C^{+2}}{2i} = -\frac{xy - qp}{2}$$
$$Q_2 = \frac{A^2 + A^{+2} + C^2 + C^{+2}}{2} = -\frac{x^2 - y^2 + q^2 - p^2}{4}$$
$$Q_3 = \frac{AC - A^+C^+}{2i} = \frac{xp + qy}{2} \tag{B3}$$

The unitary transformations whereby canonical operator x, y, q, and p can be modified and, thus, H_0 can be diagonalized are essentially three. The latter are defined by Eqs. (15), (16), and (17) representing the action of S_α (squeezing transformation), U_θ (rotation), and D_ϕ (hyperbolic transformation), respectively.

APPENDIX C: DIAGONALIZATION SCHEME FOR $v < -1/2$

The first unitary transformation is again a squeezing transformation (15) $S_\alpha = \exp(-i\alpha Q_1)$, which modifies H_0 as follows:

$$H_1' = S_\alpha H_0 S_\alpha^+ = u\sqrt{w}[x^2 + q^2 + w\,p^2 - \eta\,(xq + yp)],$$

with $w = |v| - 1/2$ and $\eta \equiv 2\tau(2/w)^{1/2}$, provided the condition $e^\alpha = \sqrt{w}$ is satisfied. The second transformation is a simple rotation $U_2 = \exp(-2i\theta J_2)$ with $\theta = \pi/4$ [see Eq. (16)] entailing

$$U_2 x U_2^+ = \frac{x+q}{\sqrt{2}}, \quad U_2 y U_2^+ = \frac{y+p}{\sqrt{2}},$$
$$U_2 q U_2^+ = \frac{q-x}{\sqrt{2}}, \quad U_2 p U_2^+ = \frac{p-y}{\sqrt{2}},$$

and

$$H_2' = U_\theta H_1' U_\theta^+ = \frac{u}{2}\sqrt{w}[(\eta+2)x^2 - (\eta-2)q^2 + (w-\eta)\,p^2 + (w+\eta)\,y^2 - 2wyp].$$

To obtain terms x^2 and q^2 with the same coefficients, we implement a second squeezing transformation $S_\beta = \exp(+i\beta Q_1)$, leading to

$$H_3' = S_\beta H_2' S_\beta^+ = \frac{u}{2}\sqrt{w}\left[\sqrt{\eta^2-4}\,(x^2-q^2) + \frac{\eta^2+2w}{\sqrt{\eta^2-4}}(y^2-p^2) + \frac{\eta(w+2)}{\sqrt{\eta^2-4}}(y^2+p^2) - 2wyp\right],$$

where parameter β must fulfill the condition

$$e^{2\beta} = \sqrt{(\eta+2)/(\eta-2)}.$$

The form of Hamiltonian H_3' is suitable for applying hyperbolic-like transformations (17) that leave terms $x^2 - q^2$ and $y^2 - p^2$ unchanged. One finds

$$H_4' = S_\phi H_3' S_\phi^+ = \frac{u}{2}\sqrt{w}\left[\sqrt{\eta^2-4}\,(x^2-q^2) + \frac{\eta^2+2w}{\sqrt{\eta^2-4}}(y^2-p^2) + \frac{2\sqrt{\eta^2(w+1)+w^2}}{\sqrt{\eta^2-4}}(y^2+p^2)\right],$$

where the condition

$$\eta(w+2)\,\mathrm{sh}(2\phi) + w\,\mathrm{ch}(2\phi)\sqrt{\eta^2-4} = 0,$$

used to eliminate the mixed term yp, provides $\mathrm{th}(2\phi) = -w\sqrt{\eta^2-4}/[\eta(w+2)]$, thereby determining parameter ϕ. We thus obtain H_4' in the form

$$H_4' = \frac{u\sqrt{w}}{2}\left[\mathcal{R}_+\left(\nu_x^2 x^2 + \frac{y^2}{\nu_x^2}\right) - \mathcal{R}_-\left(\nu_q^2 q^2 + \frac{p^2}{\nu_q^2}\right)\right]$$

with $\mathcal{R}_\pm = \sqrt{\eta^2 + 2w \pm D}$ and $D = 2\sqrt{\eta^2(w+1)+w^2}$. The explicit form of harmonic-oscillator frequencies ν_x and ν_q are defined by Eqs. (24).

APPENDIX D: ACTION OF UNITARY TRANSFORMATION W AND CALCULATION OF STANDARD DEVIATIONS

The combined action of (15), (16), and (17) gives

$$WxW^+ = e^\alpha[(C_\theta c_\phi + S_\theta s_\phi)x + (C_\theta s_\phi + S_\theta c_\phi)q]$$
$$WyW^+ = e^{-\alpha}[(C_\theta c_\phi - S_\theta s_\phi)y + (S_\theta c_\phi - C_\theta s_\phi)p],$$
$$WqW^+ = e^{-\alpha}[(C_\theta c_\phi - S_\theta s_\phi)q + (C_\theta s_\phi - S_\theta c_\phi)x]$$
$$WpW^+ = e^\alpha[(C_\theta c_\phi + S_\theta s_\phi)p - (S_\theta c_\phi + C_\theta s_\phi)y],$$

where $W = D_\phi U_\theta S_\alpha$. This results clearly shows that $\langle n,m|WfW^+|m,n\rangle = 0$ when $f = x,y,q,p$. By exploiting such transformation one easily calculates deviations $\Delta_f^2 = \langle n,m|Wf^2W^+|m,n\rangle$

$$\Delta_x^2 = \tfrac{1}{4}e^{2\alpha}[(2m+1)\gamma_x^{-2}K_{++} + (2n+1)\gamma_q^{-2}K_{-+}]$$
$$\Delta_y^2 = \tfrac{1}{4}e^{-2\alpha}[(2m+1)\gamma_x^2 K_{+-} + (2n+1)\gamma_q^2 K_{--}],$$
$$\Delta_q^2 = \tfrac{1}{4}e^{-2\alpha}[(2n+1)\gamma_q^{-2}K_{+-} + (2m+1)\gamma_x^{-2}K_{--}]$$
$$\Delta_p^2 = \tfrac{1}{4}e^{2\alpha}[(2n+1)\gamma_q^2 K_{++} + (2m+1)\gamma_x^2 K_{-+}],$$

where $K_{\delta\mu} = \mathrm{ch}(2\phi) + \delta\cos(2\theta) + \mu\,\mathrm{sh}(2\phi)\sin(2\theta)$ with $\delta = \pm$, $\mu = \pm$, $e^{2\alpha} = \sqrt{v+1/2}$ and

$$\mathrm{ch}(2\phi) = 2s\sqrt{4+\sigma^2}/\Delta, \quad \mathrm{sh}(2\phi) = (3-2v)\sigma/\Delta,$$
$$\cos(2\theta) = 2/\sqrt{4+\sigma^2}, \quad \sin(2\theta) = \sigma/\sqrt{4+\sigma^2}.$$

One should recall that $\sigma = 2\sqrt{2}\tau/\sqrt{s}$, $s = v + 1/2$, and $\Delta = 4\sqrt{s^3 + 8\tau^2(s-1)}/\sqrt{s}$, while

$$\gamma_x^2 = \sqrt{4+\sigma^2}/R_-, \quad \gamma_q^2 = \sqrt{4+\sigma^2}/R_+,$$

where $R_\pm = \sqrt{2s + \sigma^2 \pm \Delta/2}$. In view of such definitions the final form of squared deviations Δ_f^2 is given by

$$\Delta_x^2 = \frac{\sqrt{s}}{\Delta}\left[(2m+1)\frac{R_+^2 R_-}{4+\sigma^2} + (2n+1)\frac{R_-^2 R_+}{4+\sigma^2}\right]$$
$$\Delta_y^2 = \frac{1}{\sqrt{s}}\left(\frac{2m+1}{R_-\Delta}F_+ + \frac{2n+1}{R_+\Delta}F_-\right) \tag{D1}$$

with $F_\pm = 2s + \sigma^2(s-1) \pm \Delta/2$ and

$$\Delta_q^2 = \frac{2n+1}{\sqrt{s}(4+\sigma^2)\Delta}R_+F_+ + \frac{2m+1}{\sqrt{s}(4+\sigma^2)\Delta}R_-F_-$$
$$\Delta_p^2 = \frac{\sqrt{s}}{\Delta}[(2n+1)R_+ + (2m+1)R_-]. \tag{D2}$$

Concerning the regime $v < -1/2$, the calculation of $\Delta_f^2 = \langle \ell,k|Wf^2W^+|k,\ell\rangle$ is based on the more complex unitary transformation $W = D_\phi S_\beta U_2 S_\alpha$, yielding

$$WxW^+ = \frac{e^\alpha}{\sqrt{2}}[(c_\phi e^{-\beta} + s_\phi e^\beta)x + (c_\phi e^\beta + s_\phi e^{-\beta})q]$$

$$WyW^+ = \frac{e^{-\alpha}}{\sqrt{2}}[(c_\phi e^\beta - s_\phi e^{-\beta})y + (c_\phi e^{-\beta} - s_\phi e^\beta)p],$$

$$WqW^+ = \frac{e^{-\alpha}}{\sqrt{2}}[(c_\phi e^\beta - s_\phi e^{-\beta})q - (c_\phi e^{-\beta} - s_\phi e^\beta)x]$$

$$WpW^+ = \frac{e^\alpha}{\sqrt{2}}[(c_\phi e^{-\beta} + s_\phi e^\beta)p - (c_\phi e^\beta + s_\phi e^{-\beta})y],$$

where one should recall that $e^{2\alpha} = \sqrt{w}$ with $w = |v| - \frac{1}{2}$,

$$\eta = 2\sqrt{2}\tau/\sqrt{w}, \quad e^{2\beta} = [(\eta+2)/(\eta-2)]^{1/2},$$

while $c_\phi = \mathrm{ch}(\phi)$ and $s_\phi = \mathrm{sh}(\phi)$. Deviations Δ_f^2 can be shown to be function of

$$\mathrm{ch}(2\phi) = \eta(w+2)/D, \quad \mathrm{sh}(2\phi) = -w\sqrt{\eta^2-4}/D,$$

with $D = 2\sqrt{\eta^2(w+1)+w^2}$. As a consequence, deviations Δ_f^2 can written in terms of parameters η and w,

$$\Delta_x^2 = \frac{\sqrt{w}}{4}\left(\frac{2k+1}{\nu_x^2}\chi_{-+} + \frac{2\ell+1}{\nu_q^2}\chi_{++}\right)$$
$$\Delta_y^2 = \frac{1}{4\sqrt{w}}\left[(2k+1)\nu_x^2\,\chi_{+-} + (2\ell+1)\nu_q^2\,\chi_{--}\right], \tag{D3}$$

$$\Delta_q^2 = \frac{1}{4\sqrt{w}}\left(\frac{2\ell+1}{\nu_q^2}\chi_{+-} + \frac{2k+1}{\nu_x^2}\chi_{--}\right)$$
$$\Delta_p^2 = \frac{\sqrt{w}}{4}\left[(2\ell+1)\nu_q^2\,\chi_{-+} + (2k+1)\nu_x^2\,\chi_{++}\right], \tag{D4}$$

where $\chi_{rh} = (e^{r\beta} + he^{-r\beta})$, $r = \pm$, $h = \pm$, while ν_x^2 and ν_q^2 are defined by formulas (24). The explicit form of symbols χ_{rh} is

$$\chi_{-+} = \frac{2\mathcal{R}_-^2}{D\sqrt{\eta^2-4}}, \quad \chi_{++} = \frac{2\mathcal{R}_+^2}{D\sqrt{\eta^2-4}},$$

with $\mathcal{R}_\pm = \sqrt{\eta^2 + 2w \pm D}$ and

$$\chi_{+-} = 2\frac{w(\eta^2-4) + \mathcal{R}_+^2}{D\sqrt{\eta^2-4}}, \quad \chi_{--} = 2\frac{w(\eta^2-4) + \mathcal{R}_-^2}{D\sqrt{\eta^2-4}}.$$

Note that, in the limit $\epsilon = \eta^2 - 4 \to 0$, one has

$$D \simeq 2(w+2) + \epsilon\frac{w+1}{w+2}, \quad \mathcal{R}_- \simeq \frac{\sqrt{\epsilon}}{\sqrt{w+2}}, \tag{D5}$$

while $\mathcal{R}_+$ reduces to $\mathcal{R}_+ \simeq \sqrt{2(w+2)}$.

[1] K. Nemoto, C. A. Holmes, G. J. Milburn, and W. J. Munro, Phys. Rev. A **63**, 013604 (2000).
[2] R. Franzosi and V. Penna, Phys. Rev. E **67**, 046227 (2003).
[3] P. Buonsante, R. Franzosi, and V. Penna, Phys. Rev. Lett. **90**, 050404 (2003).
[4] M. Johansson, J. Phys. A: Math. Gen. **37**, 2201 (2004).
[5] G. Chong, W. Hai, and Q. Xie, Phys. Rev. E **71**, 016202 (2005).
[6] S. De Liberato and C. J. Foot, Phys. Rev. A **73**, 035602 (2006).
[7] P. Buonsante, P. G. Kevrekidis, V. Penna, and A. Vezzani, Phys. Rev. E **75**, 016212 (2007).
[8] T. F. Viscondi and K. Furuya, J. Phys. A **44**, 175301 (2011).
[9] J. A. Stickney, D. Z. Anderson, and A. A. Zozulya, Phys. Rev. A **75**, 013608 (2007).
[10] H. Hennig, J. Dorignac, and D. K. Campbell, Phys. Rev. A **82**, 053604 (2010).
[11] J. C. Eilbeck, P. S. Lomdahl, and A. C. Scott, Physica D **16**, 318 (1985).
[12] J. Carr and J. C. Eilbeck, Phys. Lett. A **109**, 201 (1985).
[13] V. M. Kenkre and D. K. Campbell, Phys. Rev. B **34**, 4959 (1986).
[14] S. Flach and C. R. Willis, Phys. Rep. **295**, 181 (1998).
[15] A. Trombettoni and A. Smerzi, Phys. Rev. Lett. **86**, 2353 (2001).
[16] P. G. Kevrekidis, D. J. Frantzeskakis, and R. Carretero-Gonzalez, *Emergent Nonlinear Phenomena in Bose-Einstein Condensates* (Springer, Berlin, 2008).
[17] R. Franzosi, R. Livi, G.-L. Oppo, and A. Politi, Nonlinearity **24**, R89 (2011)
[18] L. Cruzeiro-Hansson, H. Feddersen, R. Flesch, P. L. Christiansen, M. Salerno, and A. C. Scott, Phys. Rev. B **42**, 522 (1990).
[19] E. Wright, J. C. Eilbeck, M. H. Hays, P. D. Miller, and A. C. Scott, Physica D **69**, 18 (1993).
[20] P. Buonsante, R. Franzosi, and V. Penna, J. Phys. B **37**, S229 (2004).
[21] M. Hiller, T. Kottos, and T. Geisel, Phys. Rev. A **73**, 061604 (2006).
[22] A. R. Kolovsky, Phys. Rev. Lett. **99**, 020401 (2007).
[23] S. Mossmann and C. Jung, Phys. Rev. A **74**, 033601 (2006).
[24] F. Trimborn, D. Witthaut, and H. J. Korsch, Phys. Rev. A **79**, 013608 (2009).
[25] A. I. Streltsov, K. Sakmann, O. E. Alon, and L. S. Cederbaum, Phys. Rev. A **83**, 043604 (2011)
[26] F. D. M. Haldane, Phys. Lett. A **80**, 280 (1980).
[27] M. P. A. Fisher, P. B. Weichman, G. Grinstein, and D. S. Fisher, Phys. Rev. B **40**, 546 (1989).
[28] D. Jaksch, C. Bruder, J. I. Cirac, C. W. Gardiner, and P. Zoller, Phys. Rev. Lett. **81**, 3108 (1998).
[29] L. Amico and V. Penna, Phys. Rev. Lett. **80**, 2189 (1998).
[30] D. Ellinas, M. Johansson, and P. L. Christiansen, Physica D **134**, 126 (1999).
[31] P. Buonsante, V. Penna, and A. Vezzani, Phys. Rev. A **84**, 061601 (2011).

[32] Th. Anker, M. Albiez, R. Gati, S. Hunsmann, B. Eiermann, A. Trombettoni, and M. K. Oberthaler, Phys. Rev. Lett. **94**, 020403 (2005).

[33] M. Albiez, R. Gati, J. Fölling, S. Hunsmann, M. Cristiani, and M. K. Oberthaler, Phys. Rev. Lett. **95**, 010402 (2005).

[34] P. I. Schneider, S. Grishkevich, and A. Saenz, Phys. Rev. A **80**, 013404 (2009).

[35] I. Tikhonenkov, A. Vardi, J. R. Anglin, and D. Cohen, Phys. Rev. Lett. **110**, 050401 (2013).

[36] P. Jason, M. Johansson, and K. Kirr, Phys. Rev. E **86**, 016214 (2012).

[37] P. Buonsante, R. Franzosi, and V. Penna, J. Phys. A **42**, 285307 (2009).

[38] W.-M. Zhang, D. H. Feng, and R. Gilmore, Rev. Mod. Phys. **62**, 867 (1990).

[39] P. Buonsante and V. Penna, J. Phys. A **41**, 175301 (2008).

[40] V. Penna, Ann. Phys. **245**, 389 (1996).